Conceptual Design for Emittance Monitoring in Diamond-II

L. Bobb

Diamond-II

Introduction

*"We are now entering **a new era of scientific opportunity** with the advent of **4th generation sources**, the so-called Diffraction Limited Storage Rings...*

*The progress in accelerator technology offers the scientific community the opportunity to exploit much **brighter photon beams** and an **increased coherence over a large energy range**...*

The gains are transformative in many areas of science..."

Diamond-II Conceptual Design Report, L.C. Chapon, A.J. Dent, A. Harrison, M. Launchbury, D.I. Stuart, R.P. Walker et al., 2019

Lattice Design

4th gen. DTBA
(Double Triple Bend Achromat)

- 24 cells
- 6-fold symmetry
- Long straight every four cells
- One mid-straight in each arc

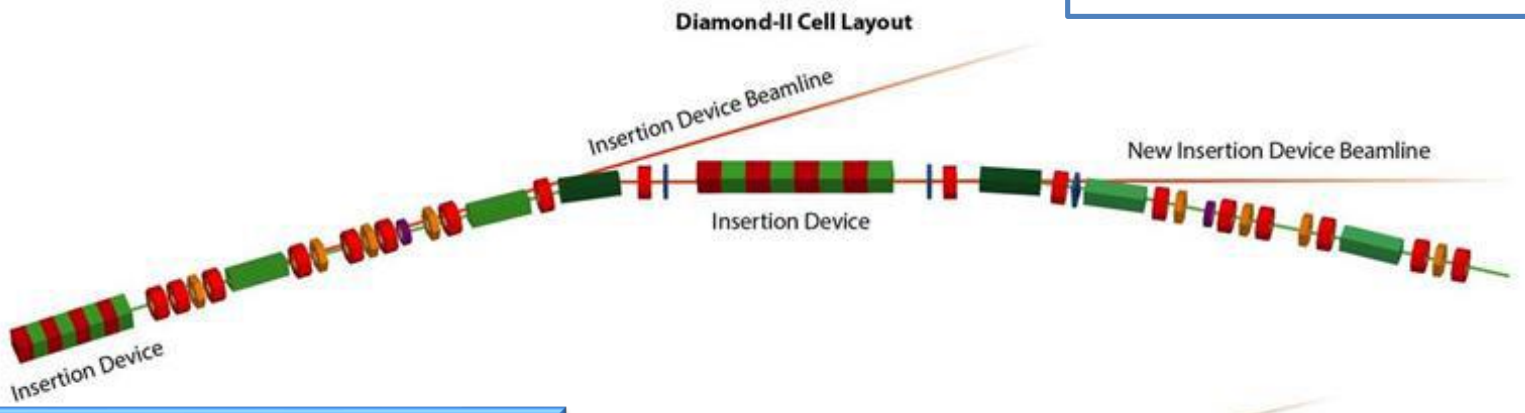

3rd gen. DBA
(Double Bend Achromat)

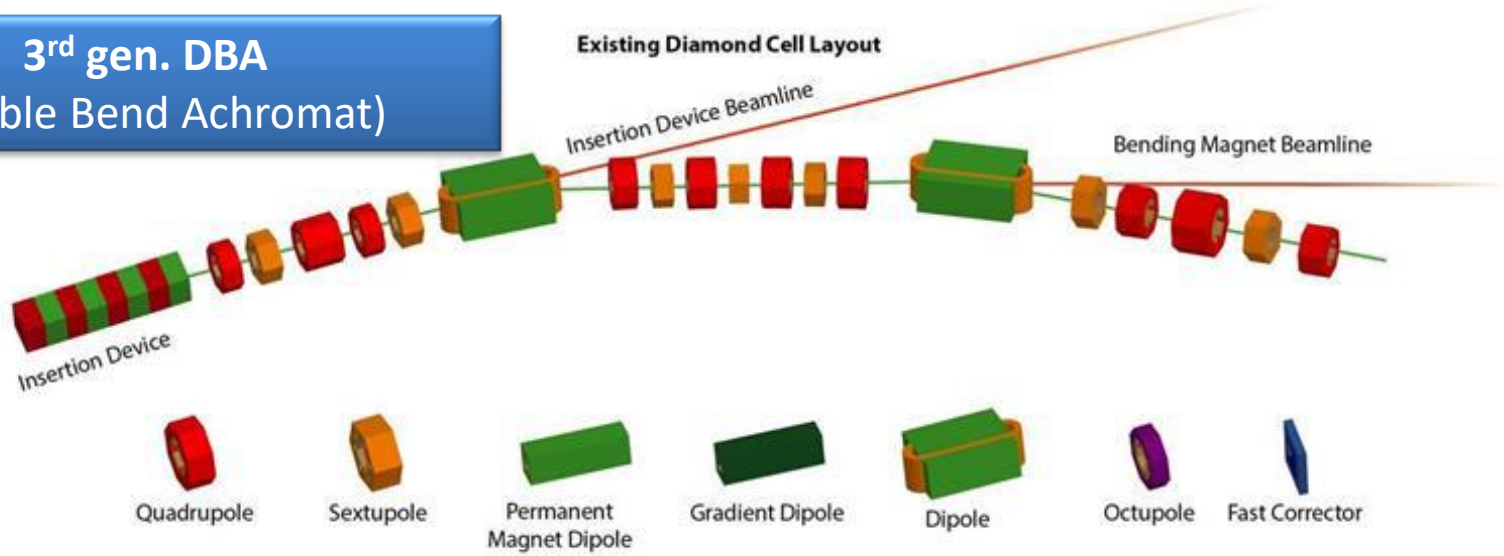

Diamond-II Conceptual Design Report, L.C. Chapon, A.J. Dent, A. Harrison, M. Launchbury, D.I. Stuart, R.P. Walker et al., 2019

Lattice Design

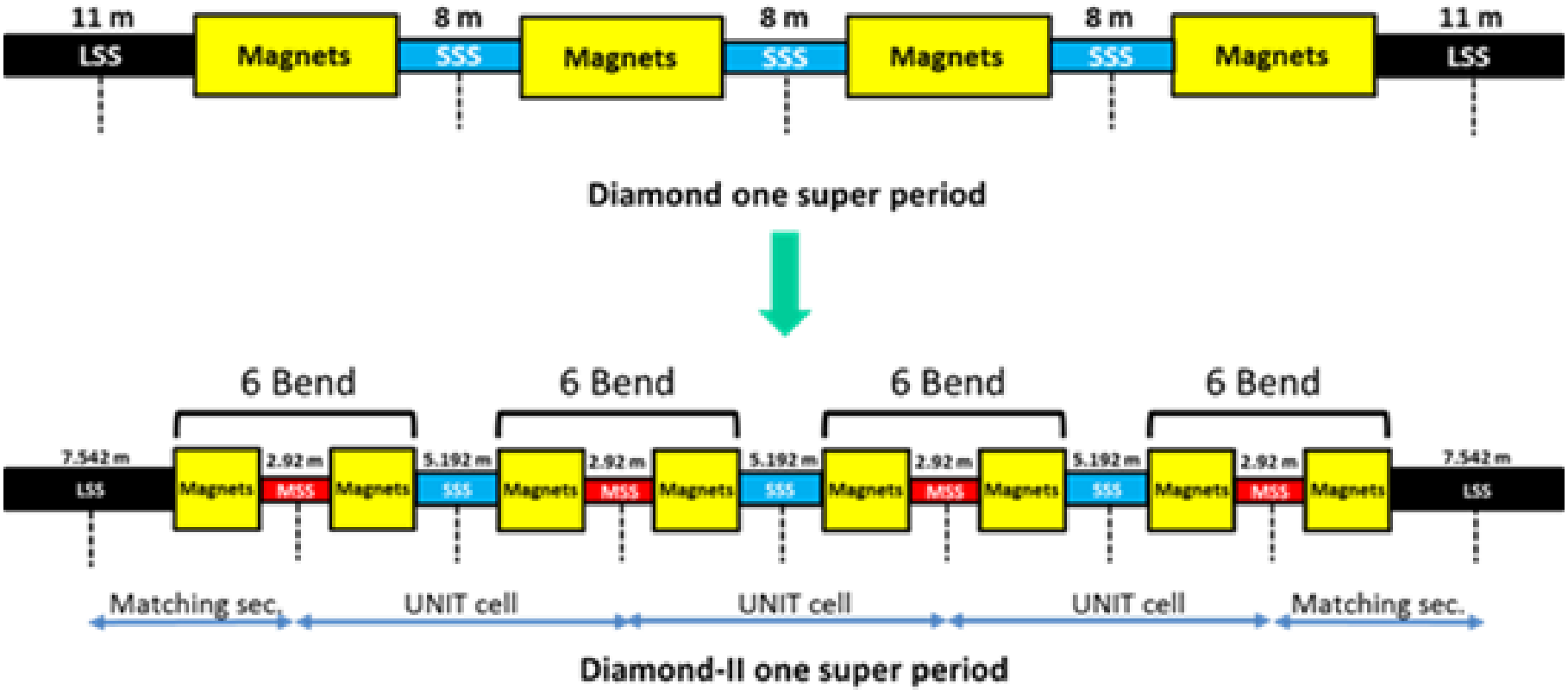

Table 2-1 : Length of the straight sections from quadrupole-to-quadrupole (hard edge model) in Diamond and Diamond-II.

Straight Section	Diamond	Diamond-II
long straight sections (LSS)	11.3 m	7.54 m
standard straight sections (SSS)	8.3 m	5.19 m
mid-straight sections (MSS)	3.4 m (DDBA)	2.92 m

Diamond-II Conceptual Design Report, L.C. Chapon, A.J. Dent, A. Harrison, M. Launchbury, D.I. Stuart, R.P. Walker et al., 2019

Lattice Constraints

The Diamond-II lattice has been designed with the **lowest possible emittance** with the constraints of:

- **doubling the number of straight sections** by including a mid-straight at the centre of each cell
- increasing the energy to **3.5 GeV**
- **maintaining** certain **minimum straight** section **lengths**
- making **minimal changes in position and angle of source points**
- preserving **off-axis injection with top-up**.

Diamond-II Conceptual Design Report, L.C. Chapon, A.J. Dent, A. Harrison, M. Launchbury, D.I. Stuart, R.P. Walker et al., 2019

Lattice Parameters (without IDs)

Table 2-8 : Main lattice parameters of Diamond and Diamond-II without IDs.

Parameter	Diamond @ 3 GeV	Diamond-II @ 3.5 GeV
Emittance [pm]	2700	160
Circumference [m]	561.571	560.574
Harmonic number	936	934
RF frequency [MHz]	499.680	499.499
Momentum compaction	1.57e-04	1.17e-04
Energy loss per turn [MeV] (dipoles)	0.988	0.670
Energy spread [%]	0.096	0.078
Horizontal damping partition	1.0014	1.3739
Vertical damping partition	1.0000	1.0000
Longitudinal damping partition	1.9986	1.6261
Horizontal damping time (ms)	11.28	14.21
Vertical damping time (ms)	11.38	19.53
Longitudinal damping time (ms)	5.71	12.01
Natural bunch length (ps)	11.55 @ 2.17 MV	9.86 @ 1.66 MV

Diamond-II Conceptual Design Report, L.C. Chapon, A.J. Dent, A. Harrison, M. Launchbury, D.I. Stuart, R.P. Walker et al., 2019

Lattice Parameters

Table 2-11 : Main lattice parameters of Diamond and Diamond-II for with the full complement of IDs.

Parameter	Diamond (all IDs)	Diamond-II (all IDs)
Emittance [pm]	3100	125
Momentum compaction	1.56e-4	1.16e-04
Energy loss per turn [MeV]	1.52	1.53
Energy spread [%]	0.10	0.10
Horizontal damping partition	1.006	1.164
Vertical damping partition	1.000	1.000
Longitudinal damping partition	1.994	1.836
Horizontal damping time (ms)	7.36	7.37
Vertical damping time (ms)	7.40	8.58
Longitudinal damping time (ms)	3.71	4.67
Natural bunch length (ps)	10.99 @ 2.80 MV	10.78 @ 2.69 MV)

Diamond-II Conceptual Design Report, L.C. Chapon, A.J. Dent, A. Harrison, M. Launchbury, D.I. Stuart, R.P. Walker et al., 2019

Comparison of Light Sources

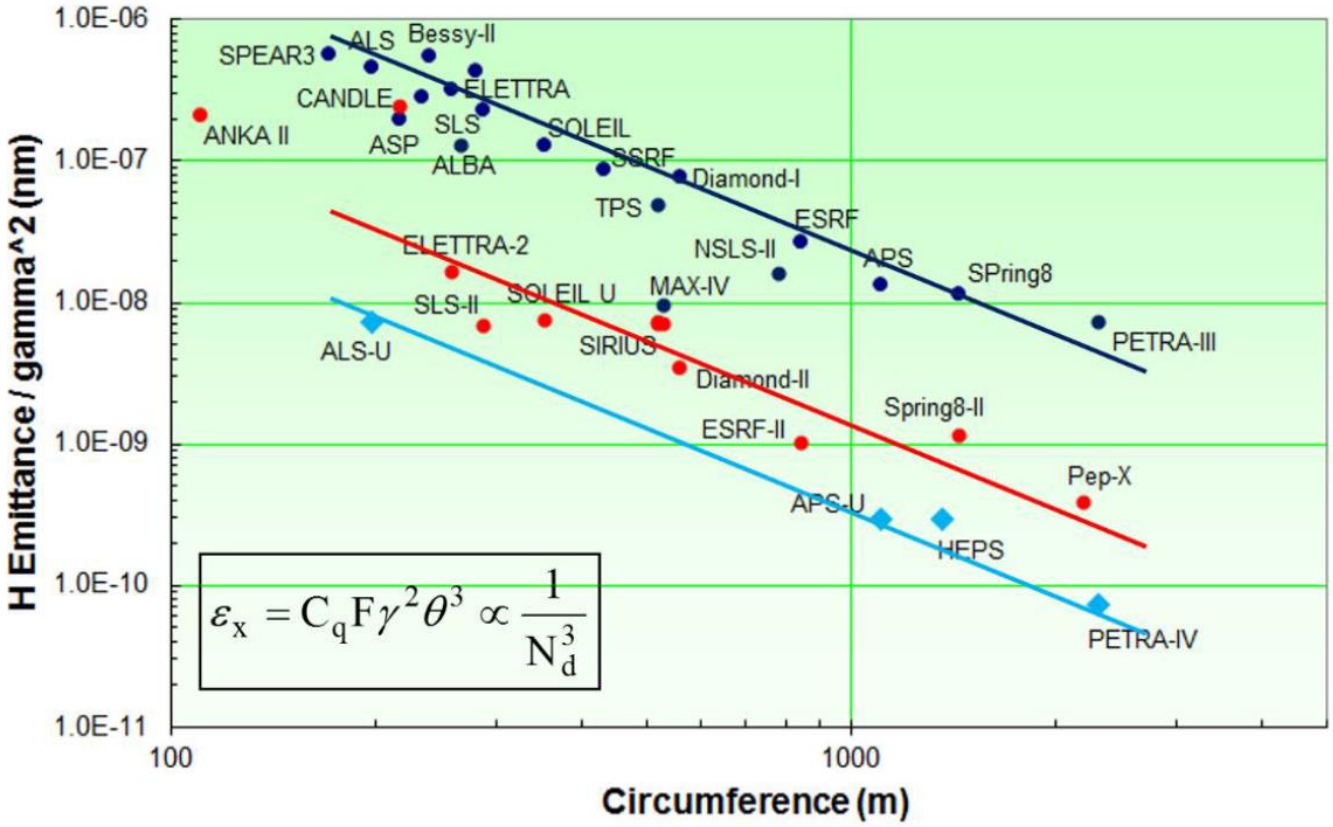

Figure 2-1 : Normalised emittance as a function of circumference: (blue) light sources in operation; (red) new projects with off-axis injection; (cyan) new projects with on-axis injection.

Diamond-II Conceptual Design Report, L.C. Chapon, A.J. Dent, A. Harrison, M. Launchbury, D.I. Stuart, R.P. Walker et al., 2019

Brightness

The figure of merit for beamlines is **Brightness: Photons/sec/mm^2/mrad^2/0.1%BW**

How to increase the brightness?

- **Increase stored beam current**
  - Increases electron beam loss rate and heating
- **Produce more photons per electron**
  - Higher electron beam energy
  - Better Insertion Devices with higher field, shorter period, more periods
- **Reduce emittance, emit more directed light**
  - For high energy photons, brightness increases inversely with horizontal and vertical emittance

Brightness

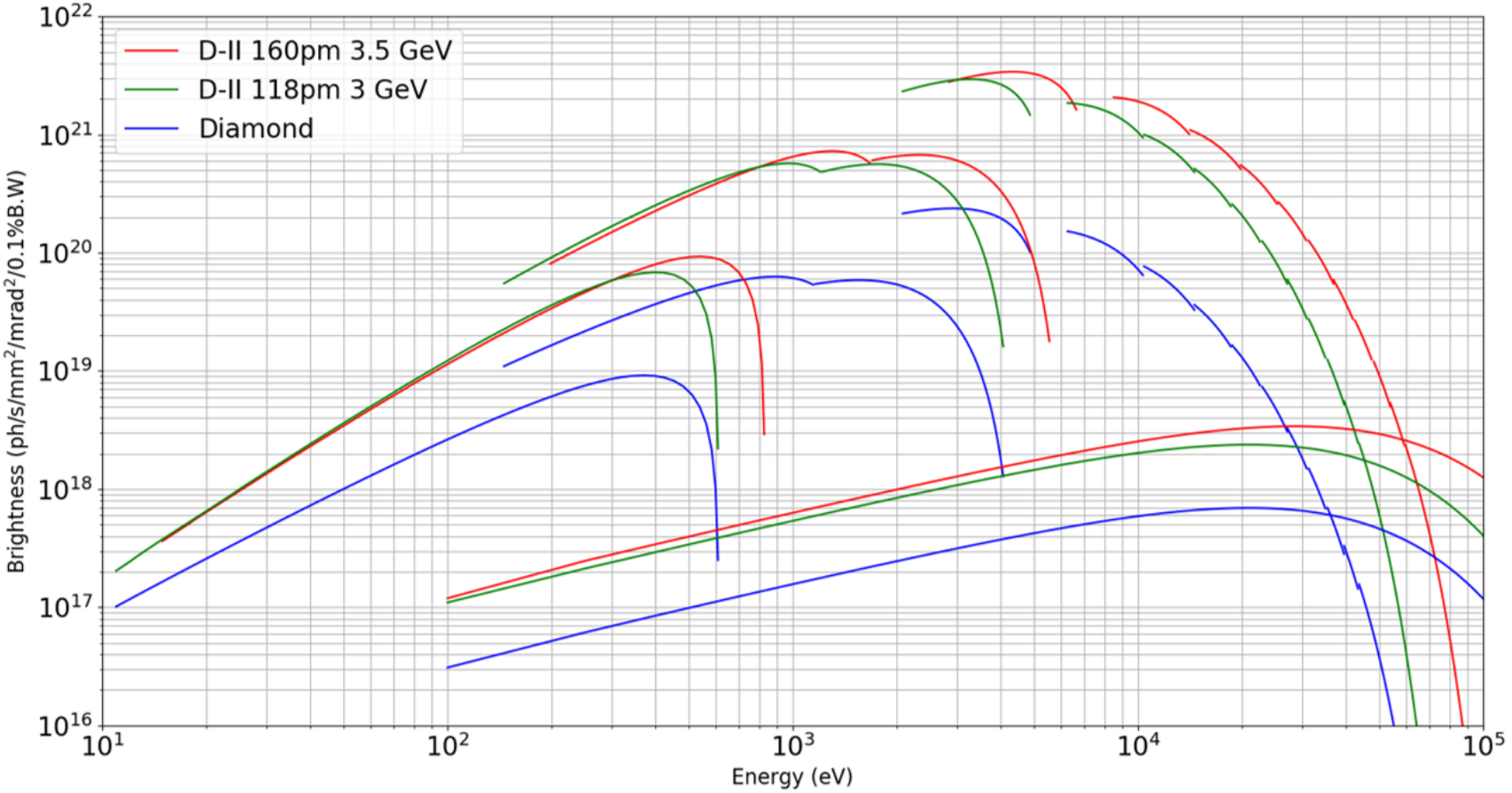

Figure 1-2 : Brightness for a set of selected sources at Diamond (blue curves), Diamond-II at 3 GeV (green curves) and Diamond-II at 3.5 GeV (red curves). In the UV regime, soft X-ray regime and hard X-ray, the brightness curves are shown respectively for the I05, I21, the future CPMU 15.6 mm period (to be installed on I11 and VMXm), and for the superconducting wiggler on I12 (JEEP). All calculations have been made with Spectra 9 using the Wigner function. A phase error of 3° for the undulators has been taken into account analytically.

Diamond-II Conceptual Design Report, L.C. Chapon, A.J. Dent, A. Harrison, M. Launchbury, D.I. Stuart, R.P. Walker et al., 2019

Coherent Fraction

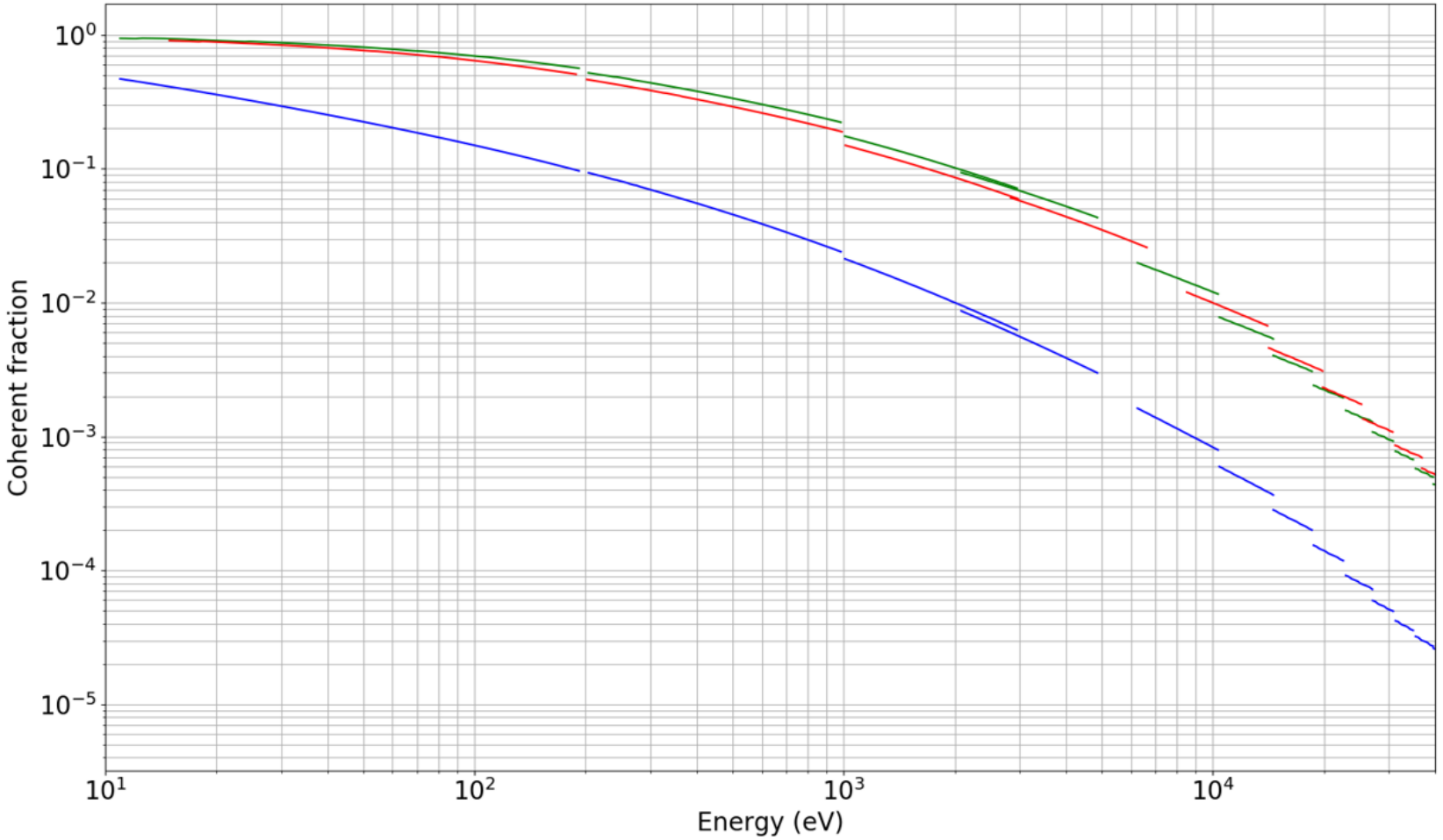

Figure 1-3 : Coherent fraction in the horizontal direction as a function of Energy for Diamond (blue), Diamond-II at 3 GeV (green) and Diamond-II at 3.5 GeV (red). All curves have been produced with Spectra using the Wigner function and approximating the coherent fraction as the ratio between the Brightness and the Brightness calculated in the limit of zero emittance and zero energy spread.

Diamond-II Conceptual Design Report, L.C. Chapon, A.J. Dent, A. Harrison, M. Launchbury, D.I. Stuart, R.P. Walker et al., 2019

Diagnostics Requirements

General requirements:

- State-of-the-art diagnostics
- Active feedback (even more than what we have in Diamond!)
- Beam stability over a larger frequency range and given the reduced fractional beam size.

Table 2-51 : Some parameters relevant to diagnostics in Diamond and Diamond-II

Parameter	Diamond (2019)	Diamond-II
Emittance H/V	2700 pm / 8 pm	160 pm / 8 pm
BPM block aperture H/V	80 mm / 22 mm	20 mm round
Number of BPMs	175	252
Beam size at source H/V (standard straight)	123 μm / 3.5 μm	30 μm / 4 μm
Orbit stability relative	10% of H/V size to 100 Hz	3% of H/V size to 1000 Hz
Orbit stability absolute (centre of standard straight)	12 μm / 0.35 μm	0.9 μm / 0.12 μm

Diamond-II Conceptual Design Report, L.C. Chapon, A.J. Dent, A. Harrison, M. Launchbury, D.I. Stuart, R.P. Walker et al., 2019

Brief Summary of Diamond-II

- Beamlines:
  - Insertion Device beamlines are retained in their existing locations
  - Bending magnet beamlines are upgraded to Insertion Devices
  - Additional new beamlines in the mid-straights

- To increase the brightness:
  - The beam energy is increased to 3.5 GeV (requires a new booster).
  - The beam emittance is reduced.
  - The beam current remains the same (300 mA)

- Diamond-II will provide orders of magnitude improvement in resolution in time and space on beamlines (see Diamond-II Science Case).
  - Enabling new types of measurements
  - “Proof of principle” experiments become routine experiments
  - Higher throughput

- Dark time from 7 April 2025 until 7 Oct 2026 (back to users)

Diamond-II Conceptual Design Report, L.C. Chapon, A.J. Dent, A. Harrison, M. Launchbury, D.I. Stuart, R.P. Walker et al., 2019

Emittance Monitoring

Emittance Requirements

The emittance monitoring deployed for Diamond-II should:

- provide measurements of the **horizontal and vertical emittances** $\varepsilon_{x,y}$ and **energy spread** σ_E of the electron beam in the storage ring
- consist of **at least two transverse beam size monitors**, which are **located at positions** in the storage ring **with different lattice parameters**, specifically dispersion
- operate at an acquisition rate and robustness **suitable for continuous feedback systems**
- ideally be **distributed around the ring to provide global monitoring** of the transverse profile of the electron beam.

Diamond-II Conceptual Design Report, L.C. Chapon, A.J. Dent, A. Harrison, M. Launchbury, D.I. Stuart, R.P. Walker et al., 2019

Absolute Beam Profile Measurement

Transverse profile of the electron beam will be measured using X-ray Pinhole Cameras (XPCs)

Source−to−scintillator magnification $|M_1| = \left|-\frac{d_i}{d_o}\right|$

Scintillator−to−camera magnification $|M_2| \sim 1$

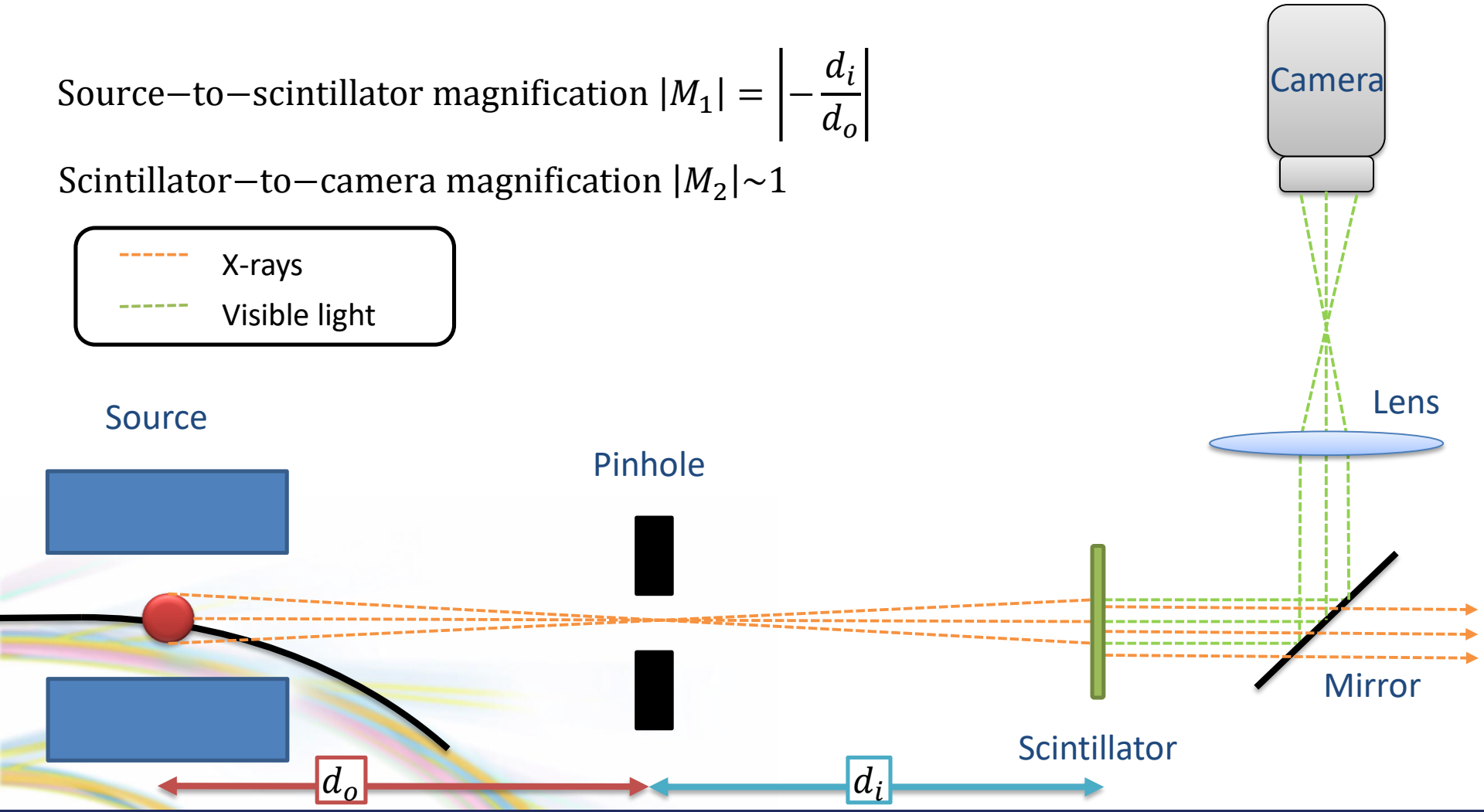

Point Spread Function

Measured beam size is a convolution of the true beam size and the PSF (Gaussian approx.):

$$\sigma^2_{Measured} = \sigma^2_{True} + \sigma^2_{PSF}$$

where

$$\sigma^2_{PSF} = \sigma^2_{Pinhole} + \sigma^2_{Camera} > 0$$

$$\sigma^2_{Pinhole} = \sigma^2_{Diffraction} + \sigma^2_{Aperture}$$
$$\sigma^2_{Camera} = \sigma^2_{Screen} + \sigma^2_{Lens} + \sigma^2_{Sensor}$$

P. Elleaume et al., J. Synchrotron Radiat. 2, 209 (1995).
C. Thomas et al., Phys. Rev. ST Accel. Beams 13, 022805, (2010).

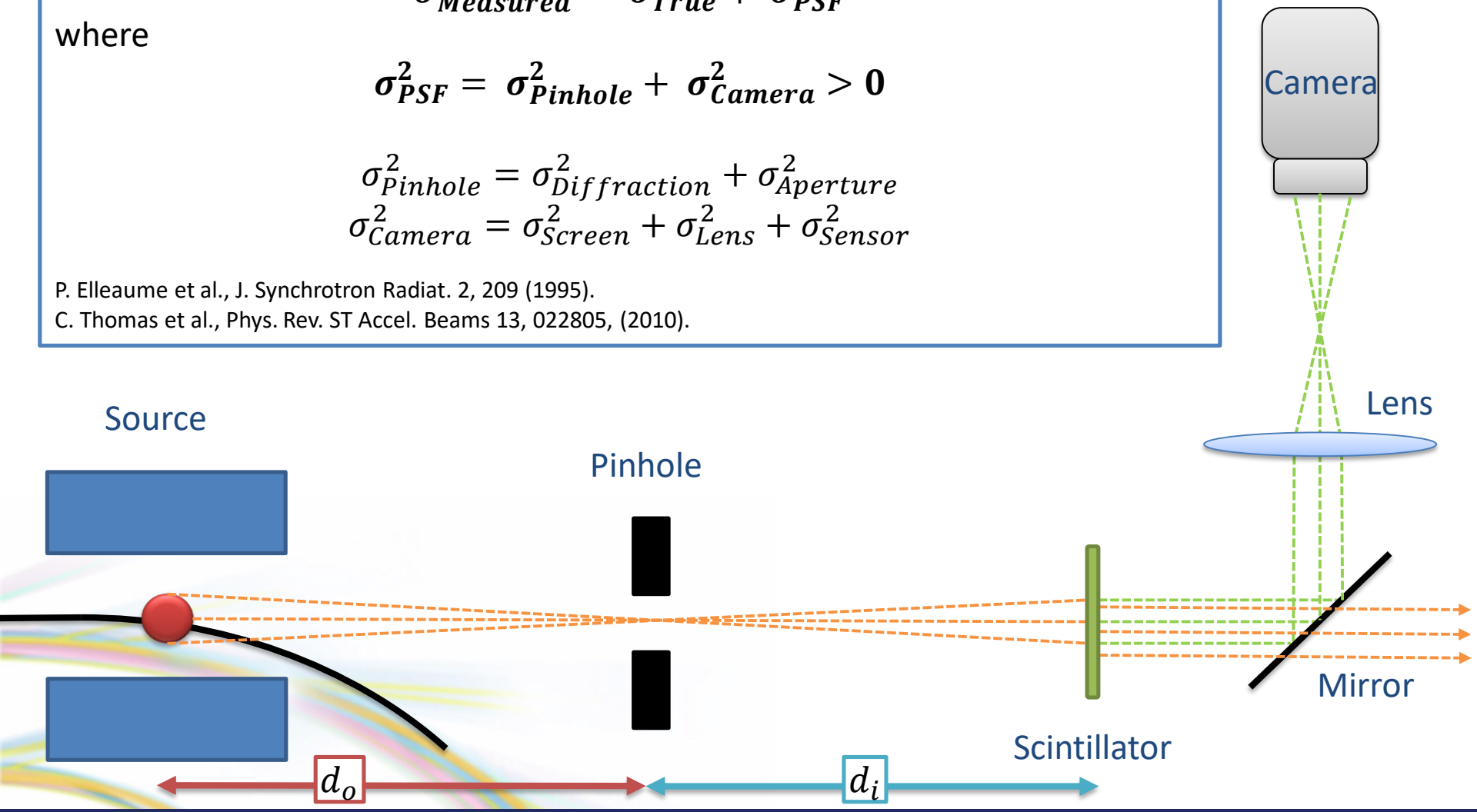

Why X-ray Pinhole Cameras?

- **Provide a direct image** of the transverse beam profile
- **Simple to align** and operate on day 1
- **Easy to maintain**
- **Years of experience** using XPCs at Diamond
- **Suitable for feedback** (already used for Vertical Emittance feedback).
- **Sufficient spatial resolution**
- Allows the sanity checking of other diagnostic instrumentation.
- **Affordable**

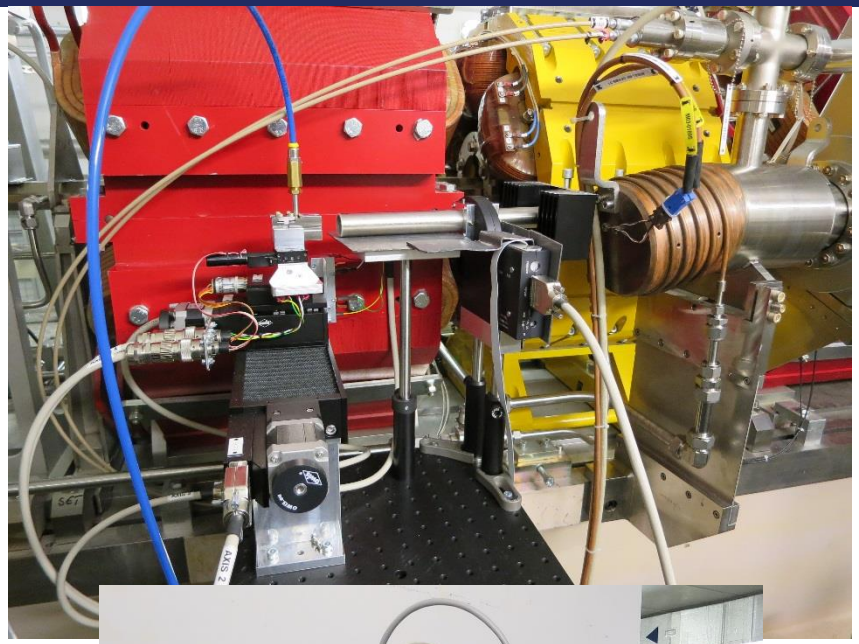

Dual Purpose Diagnostic

Emittance Monitoring + **CCTV**

While we have human operators, the importance of easy human interpretation shouldn't be overlooked.

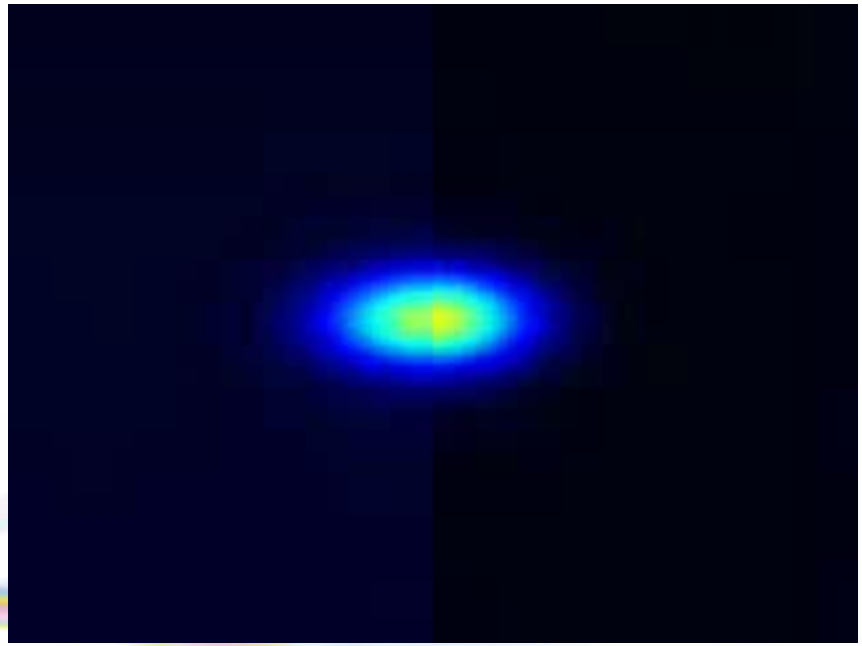

Injection at Diamond 2015

TMBF at Diamond 2015

Courtesy of the Diagnostics Group

Dual Purpose Diagnostic

Emittance Monitoring + **CCTV**

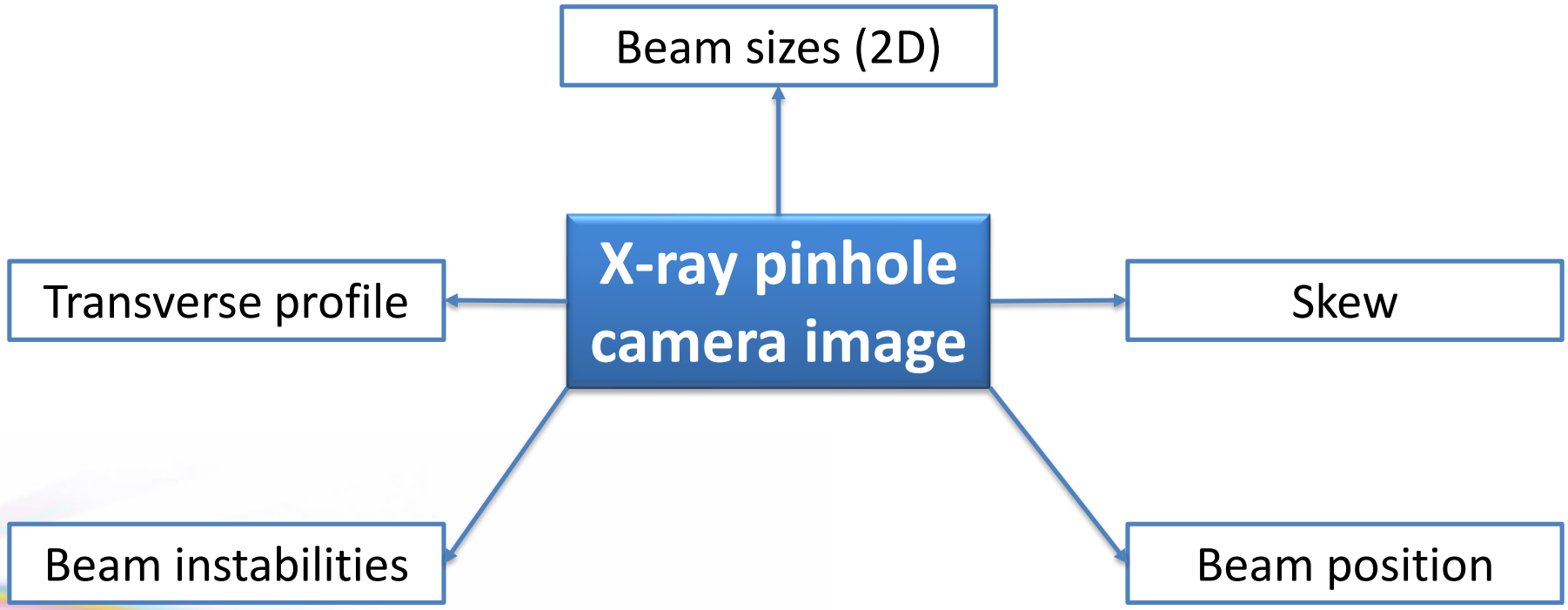

Emittance Calculation

Using two pinhole cameras at different locations:

1. Fit a 2D Gaussian to obtain horizontal and vertical imaged sizes $\sigma_{x_{1,2}}^{image}$ and $\sigma_{y_{1,2}}^{image}$ respectively.

2. Deconvolve and scale using magnification to obtain the electron beam sizes e.g. Gaussian subtraction in quadrature:

$$\sigma_{y_1} = \frac{\sqrt{(\sigma_{y_1}^{image})^2 - \sigma_{PSF}^2}}{M_1}$$

3. Given the lattice parameters, solve the following matrix equation to obtain the horizontal and vertical emittances $\varepsilon_{x,y}$, and energy spread σ_e:

$$\begin{bmatrix} \sigma_{x_1}^2 \\ \sigma_{x_2}^2 \\ \sigma_{y_1}^2 \\ \sigma_{y_2}^2 \end{bmatrix} = \begin{bmatrix} \beta_{x_1} & 0 & \eta_{x_1}^2 \\ \beta_{x_2} & 0 & \eta_{x_2}^2 \\ 0 & \beta_{y_1} & \eta_{y_1}^2 \\ 0 & \beta_{y_2} & \eta_{y_2}^2 \end{bmatrix} \begin{bmatrix} \varepsilon_x \\ \varepsilon_y \\ \sigma_e^2 \end{bmatrix}$$

VEFB Operation at Diamond

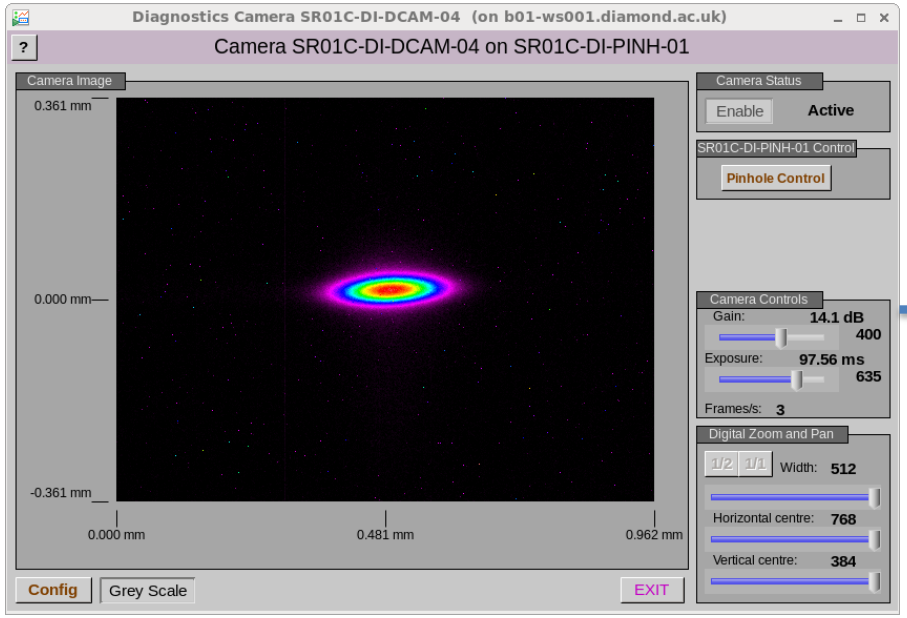

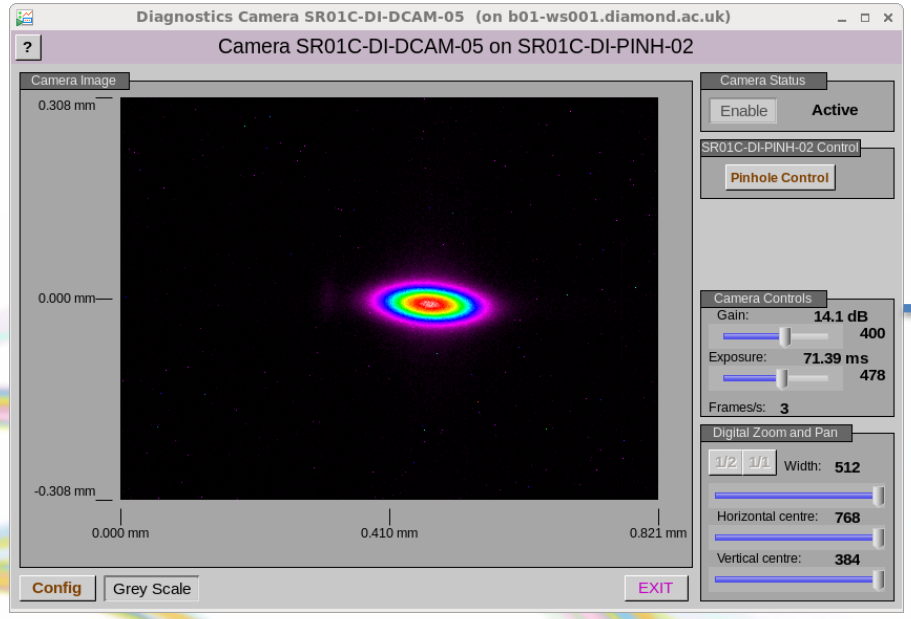

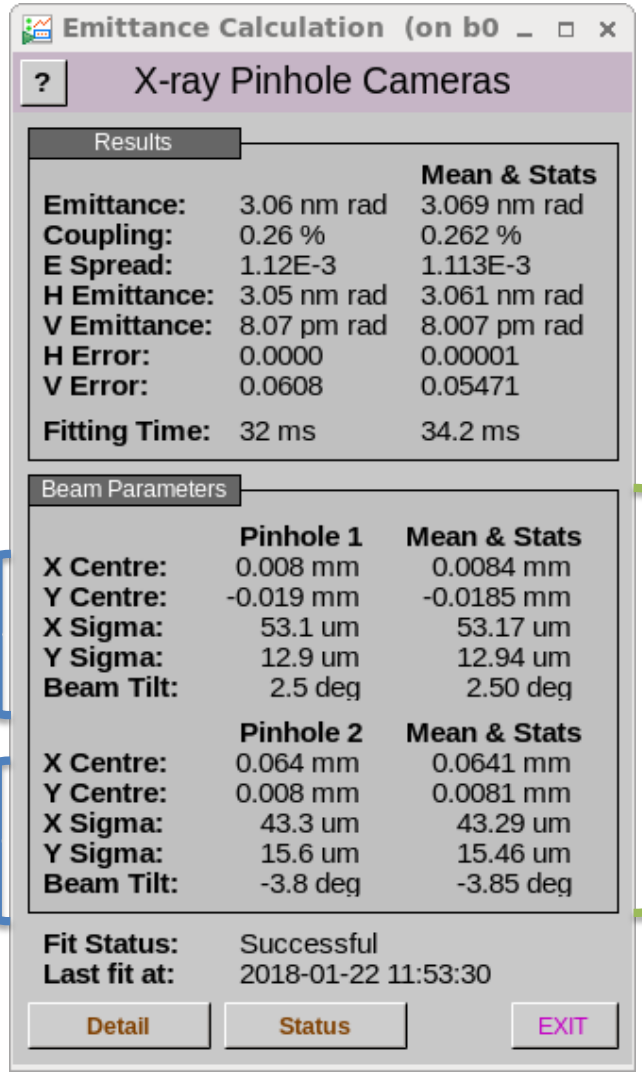

Diamond-II Source Points

OLD DRAWING

DII - MAGNET SET TYPE LM
(LM = LONG STRAIGHT TO MID-STRAIGHT)

N°	DRG N°	DESCRIPTION	QTY	REMARKS
1	1141235_A	DTBA M-H6BA/ SEXTUPOLE ASSY 100LG	1	
2	1141235_AA	DIPOLE VESSEL TYPE 1 - ENVELOPE	1	
3	1141235_AC	DII DQ DIPOLE (ELECTRO-MAGNET) 14/08/18	1	
4	1141235_AD	DIPOLE VESSEL TYPE 2 - ENVELOPE	1	
5	1141235_AE	DIPOLE VESSEL TYPE 2 - ENVELOPE	1	
6	1141235_C	DTBA M-H6BA/ SEXTUPOLE ASSY 140LG	3	
7	1141235_E	DTBA M-H6BA/ SEXTUPOLE / CORRECTOR ASSY 100LG	1	
8	1141235_G	DTBA M-H6BA/ QUADRUPOLE ASSY 125LG	3	
9	1141235_J	DTBA M-H6BA/ QUADRUPOLE ASSY 142LG	3	
10	1141235_K	DTBA M-H6BA/ QUADRUPOLE ASSY 162LG	1	
11	1141235_O	DTBA M-H6BA/ QUADRUPOLE ASSY 250LG	1	
12	1141235_Q	DTBA M-H6BA/ QUADRUPOLE ASSY 350LG	1	
13	1141235_S	DTBA M-H6BA/ CORRECTOR ASSY 100LG	2	
14	1141235_T	DIAMOND 2 BPM TO BE FULLY DEFINED	6	
15	1141235_U	DL DIPOLE NEW 20.08.18	2	
16	1141235_V	DII OCTUPOLE MAGNET	1	

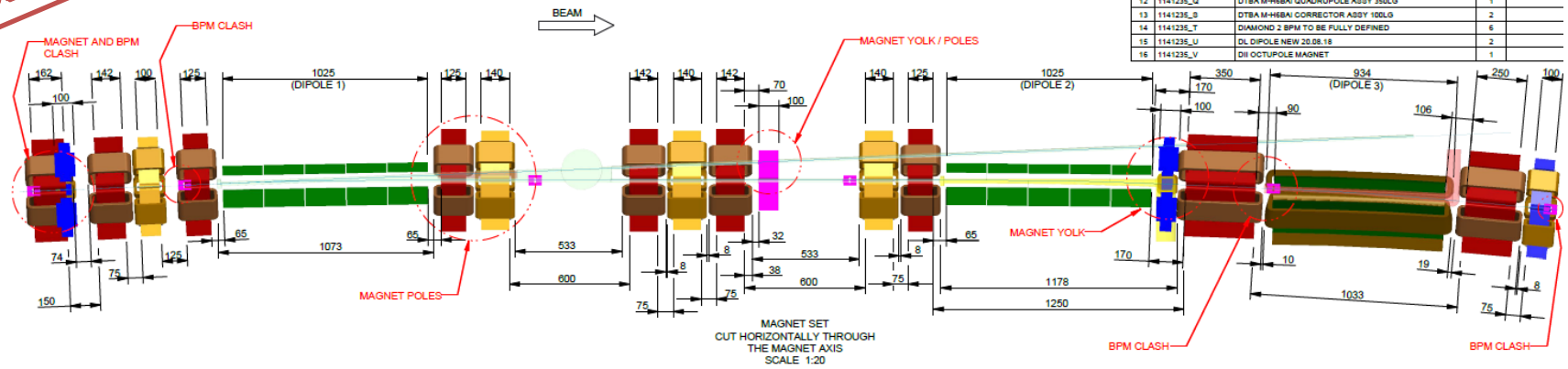

DII - MAGNET SET TYPE MS
(MS = MID-STRAIGHT TO STANDARD STRAIGHT)

N°	DRG N°	DESCRIPTION	QTY	REMARKS
1	1141235_A	DTBA M-H6BA/ SEXTUPOLE ASSY 100LG	1	
2	1141235_AC	DII DQ DIPOLE (ELECTRO-MAGNET) 14/08/18	1	
3	1141235_AF	DIPOLE VESSEL TYPE 1 - ENVELOPE	1	
4	1141235_AG	DIPOLE VESSEL TYPE 2 - ENVELOPE	1	
5	1141235_AH	DIPOLE VESSEL TYPE 2 - ENVELOPE	1	
6	1141235_C	DTBA M-H6BA/ SEXTUPOLE ASSY 140LG	3	
7	1141235_E	DTBA M-H6BA/ SEXTUPOLE / CORRECTOR ASSY 100LG	1	
8	1141235_G	DTBA M-H6BA/ QUADRUPOLE ASSY 125LG	3	
9	1141235_J	DTBA M-H6BA/ QUADRUPOLE ASSY 142LG	2	
10	1141235_M	DTBA M-H6BA/ QUADRUPOLE ASSY 175LG	1	
11	1141235_O	DTBA M-H6BA/ QUADRUPOLE ASSY 250LG	1	
12	1141235_Q	DTBA M-H6BA/ QUADRUPOLE ASSY 350LG	1	
13	1141235_S	DTBA M-H6BA/ CORRECTOR ASSY 100LG	1	
14	1141235_T	DIAMOND 2 BPM TO BE FULLY DEFINED	5	
15	1141235_U	DL DIPOLE NEW 20.08.18	2	
16	1141235_V	DII OCTUPOLE MAGNET	1	

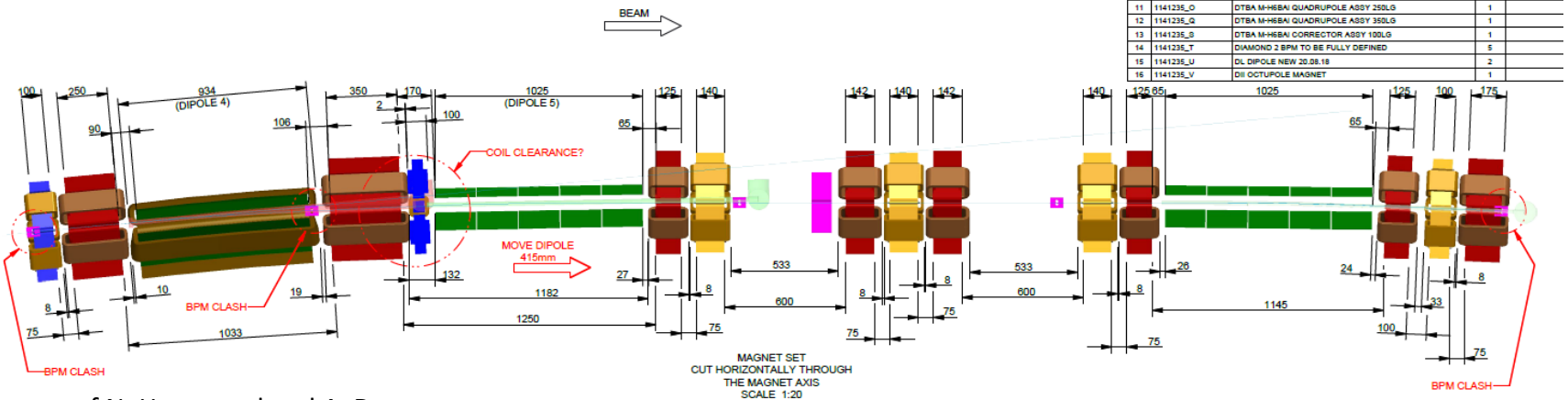

Courtesy of N. Hammond and A. Day

Source Point Comparison

Table 2-52 : Source point properties, beam size contributions and available power.

Parameter	DLS-I: BM	D1: Long	D1: Standard	D4	Mid Straight 3PW
β_x [m]	0.84	1.43	1.46	0.27	2.4
β_y [m]	20.34	18.97	13.46	16.13	1.15
η_x [m]	14.44	0	0.1	6.4	24.6
ε_x [pm]	3200	150			
ε_y [pm]	8	8			
σ_E [%]	0.107	0.078			
H beam size from emittance [μm]	51.8	14.6	14.8	6.4	19.0
H beam size from energy spread [μm]	15.4	0	0.1	5	19.2
Total H beam size [μm]	54	14.6	14.8	8	27
V beam size from emittance [μm]	12.8	12.3	10.4	11.4	3
Available power in 250 μrad [mW]	70	31	31	24	264

Diamond-II Conceptual Design Report, L.C. Chapon, A.J. Dent, A. Harrison, M. Launchbury, D.I. Stuart, R.P. Walker et al., 2019

Spectral Power Distribution

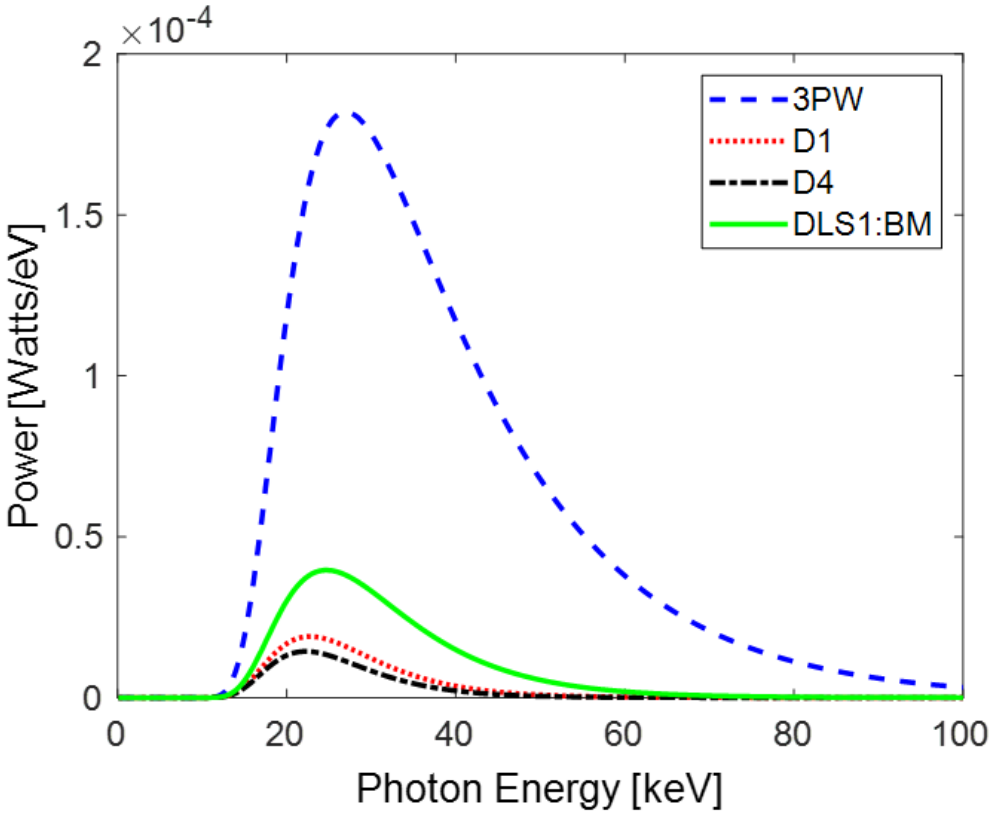

Figure 2-132 : Comparison of the transmitted spectral power distribution through a 1 mm aluminium window and 10m of air for dipoles 1, 4, 3PW and a Diamond bending magnet.

Diamond-II Conceptual Design Report, L.C. Chapon, A.J. Dent, A. Harrison, M. Launchbury, D.I. Stuart, R.P. Walker et al., 2019

Source Point Selection

It is observed that:

- the **most suitable source for emittance measurement is D1 from both long and standard straights** because the energy spread contribution to the total horizontal beam size is negligible
- in addition to D1, **the most suitable source for energy spread measurement** would be the **3PW on the mid-straight** due to the larger dispersion
- the **D4 source point would also be suitable for both emittance and energy spread** measurements in addition to X-ray pinhole cameras on D1 due to large dispersion in comparison to the horizontal beta function, but with a more challenging horizontal beam size.
- the pinhole can be located closer to the dipole source points, such that the **source-to-screen magnification is increased** to approximately 4.5 which is almost two times greater than in Diamond (mag=2.5).

Diamond-II Conceptual Design Report, L.C. Chapon, A.J. Dent, A. Harrison, M. Launchbury, D.I. Stuart, R.P. Walker et al., 2019

Design Phase

Tasks to be completed during the detailed design phase:

- Decide on the sources to use and design the dipole/crotch vessels accordingly.
- Decide whether a common vessel design suitable for all locations is possible.
- Decide on the number of X-ray pinhole cameras to be installed
- Decide on the details of beam extraction to air.
- Choose pinhole size, method of fabrication, suitable support and actuation.
- Choose detection system: direct X-ray or scintillation screen, lens, camera; readout and processing

Diamond-II Conceptual Design Report, L.C. Chapon, A.J. Dent, A. Harrison, M. Launchbury, D.I. Stuart, R.P. Walker et al., 2019

Other Diagnostics

Summary of Topical Workshop:
Emittance Measurements
for Synchrotron Light Sources and FELs

Ubaldo Iriso (ALBA-CELLS),
F. Ewald (ESRF), G. Kube (DESY), T. Mitsuhashi (KEK),
V. Schlott (PSI) and K. Wittenburg (DESY)

Summary of ε- meas for SLS

Presentations are available at: https://indico.cells.es/indico/event/128

Technique	Smallest σ, μm (measured)	Workshop Talk
X-ray Pinhole	7	L. Bobb / F. Ewald
Compound Refractive Lenses	10	F. Ewald / A. Snigirev
In-air X-ray Detectors	9	F. Ewald
Vis. Light Interf.	3.9	T. Mitsuhashi
Vis. Light Inter. (Rotating Mask)	2 (sim)	L. Torino
π-polarization (vis)	3.7	A. Andersson
Coded Aperture	5	J. Flanagan
X-ray Diffraction	4.8	A. Snigirev
X-ray (multi/lens) Interferometry	4.8	A. Snigirev
HNFS	110	M. Siano

In-air X-ray Detectors

Table 1: Comparison of X-ray pinhole cameras and X-ray Projection Monitors.

	XPC	XPM
Beam size measurement	σ_x and σ_y	σ_y only
Distance required from source point	> 15 m	< 2 m
Spatial resolution primarily depends on	Magnification	Photon Energy

B.K. Scheidt et al., Proc. of DIPAC 2007, TUPB08, 72-74.

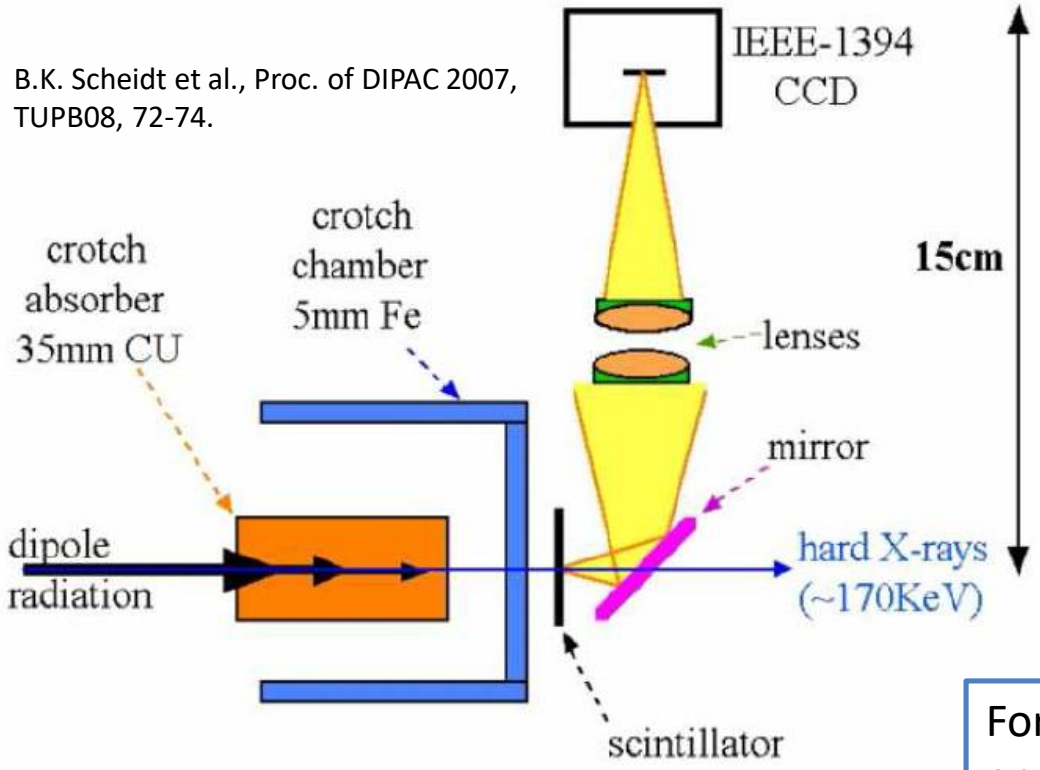

Photon Energy [keV]	PSF_{FWHM} [μm]	$\frac{PSF_{FWHM}}{\sigma_{yFWHM}}$
40	72	3.4
50	64	3.0
60	58	2.7
70	54	2.5
80	50	2.4
90	47	2.2
100	45	2.1
110	43	2.0
120	41	1.9
130	39	1.8
140	38	1.8
150	36	1.7

For required spatial resolution, photon energies >100 keV are needed.

→ Not feasible in Diamond-II

Visible Synchrotron Radiation

It would be preferable to have complementary monitors available.

Visible synchrotron radiation (SR) has the obvious advantage of accessibility in comparison to X-ray instrumentation.

With a new visible light extraction and propagation path to preserve the wavefront, other techniques become feasible:

- Interferometry
- π-polarisation

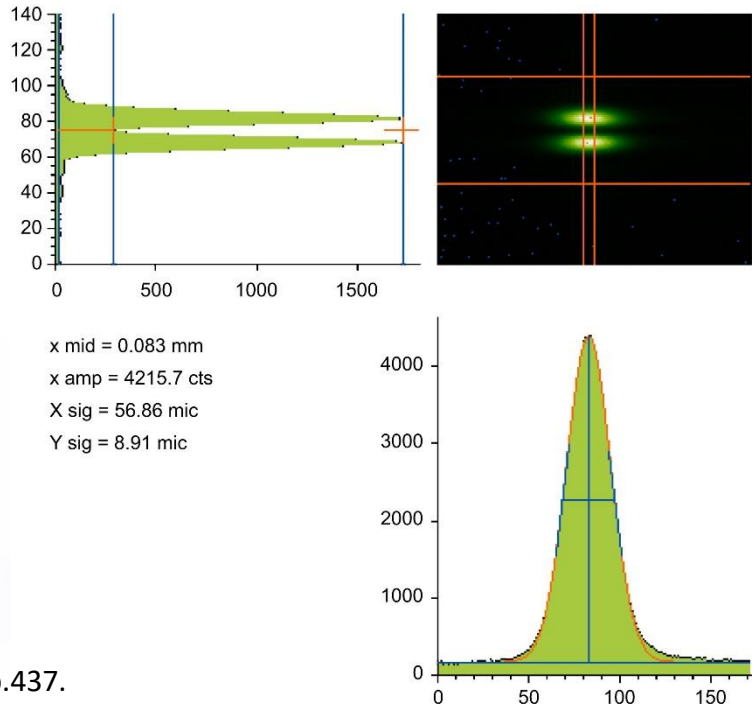

A. Andersson et al., Nucl. Inst. and Meth. A, 591 (2008), p.437.

Conclusion

- Many **3rd generation light sources** are planning or undergoing **upgrades**.
- With these **MBA lattices**, the beam **emittance is reduced** which improves the brightness on beamlines.
- **Emittance monitoring** remains **a crucial diagnostic** for operation but is likely to be **more challenging** to measure depending upon the availability of suitable source points e.g. SR extraction, beta functions and dispersion.
- **Collaborative efforts are welcome**, to enable the discussion of new ideas and improve emittance measurement in these future machines!

Acknowledgements

Special thanks to Guenther Rehm and the Diagnostics Group.

Thanks to the following authors for their contributions to the Diamond-II CDR:

C. Abraham, L. Alianelli, M. Apollonio, R. Bartolini, C. Bloomer, L. Bobb, L.C. Chapon, C. Christou, P. Coll, M.P. Cox, A.J. Dent, S.S. Dhesi, S. Diaz-Moreno, G. Evans, R. Doull, R. Fielder, H. Ghasem, D.R. Hall, N.P. Hammond, A. Harrison, M.T. Heron, J. Hriljac, S.E. Hughes, J. Kay, V.C. Kempson, S.A. Macdonell, I. Martin, S.R. Milward, A. Morgan, C.L. Nicklin, T. Olsson, M. Popkiss, P. Quinn, R. Rambo, G. Rehm, A. Rose, K.J. Sawhney, S.M. Scott, A. Shahveh, N. Tartoni, R.P. Walker, M.A. Walsh

and to the editors:

L.C. Chapon, A.J. Dent, A. Harrison, M. Launchbury, D.I. Stuart, R.P. Walker

Thank you for your attention!

Extra Slides

Touschek Lifetime

Table 2-24 : Average Touschek lifetime and total lifetime for the bare lattice. The Touschek lifetimes with harmonic cavity are for the Super-3HC harmonic cavity tuned according to the settings in Table 2-20 and including the transient beam loading in 8 normal conducting main cavities operated at optimal power coupling and detuning.

	Average Touschek lifetime	Total lifetime activated NEG	Total lifetime saturated NEG
No HC	0.95 ± 0.12 h	0.95 ± 0.12 h	0.93 ± 0.11 h
With HC, uniform fill	4.37 ± 0.56 h	4.32 ± 0.55 h	3.96 ± 0.46 h
With HC, standard mode	1.91 ± 0.24 h	1.90 ± 0.24 h	1.83 ± 0.22 h

Point Spread Function

Measured beam size is a convolution of the true beam size and the PSF (Gaussian approx.):

$$\sigma^2_{Measured} = \sigma^2_{True} + \sigma^2_{PSF}$$

where

$$\sigma^2_{PSF} = \sigma^2_{Pinhole} + \sigma^2_{Camera} > 0$$

$$\sigma^2_{Pinhole} = \sigma^2_{Diffraction} + \sigma^2_{Aperture}$$
$$\sigma^2_{Camera} = \sigma^2_{Screen} + \sigma^2_{Lens} + \sigma^2_{Sensor}$$

P. Elleaume et al., J. Synchrotron Radiat. 2, 209 (1995).
C. Thomas et al., Phys. Rev. ST Accel. Beams 13, 022805, (2010).

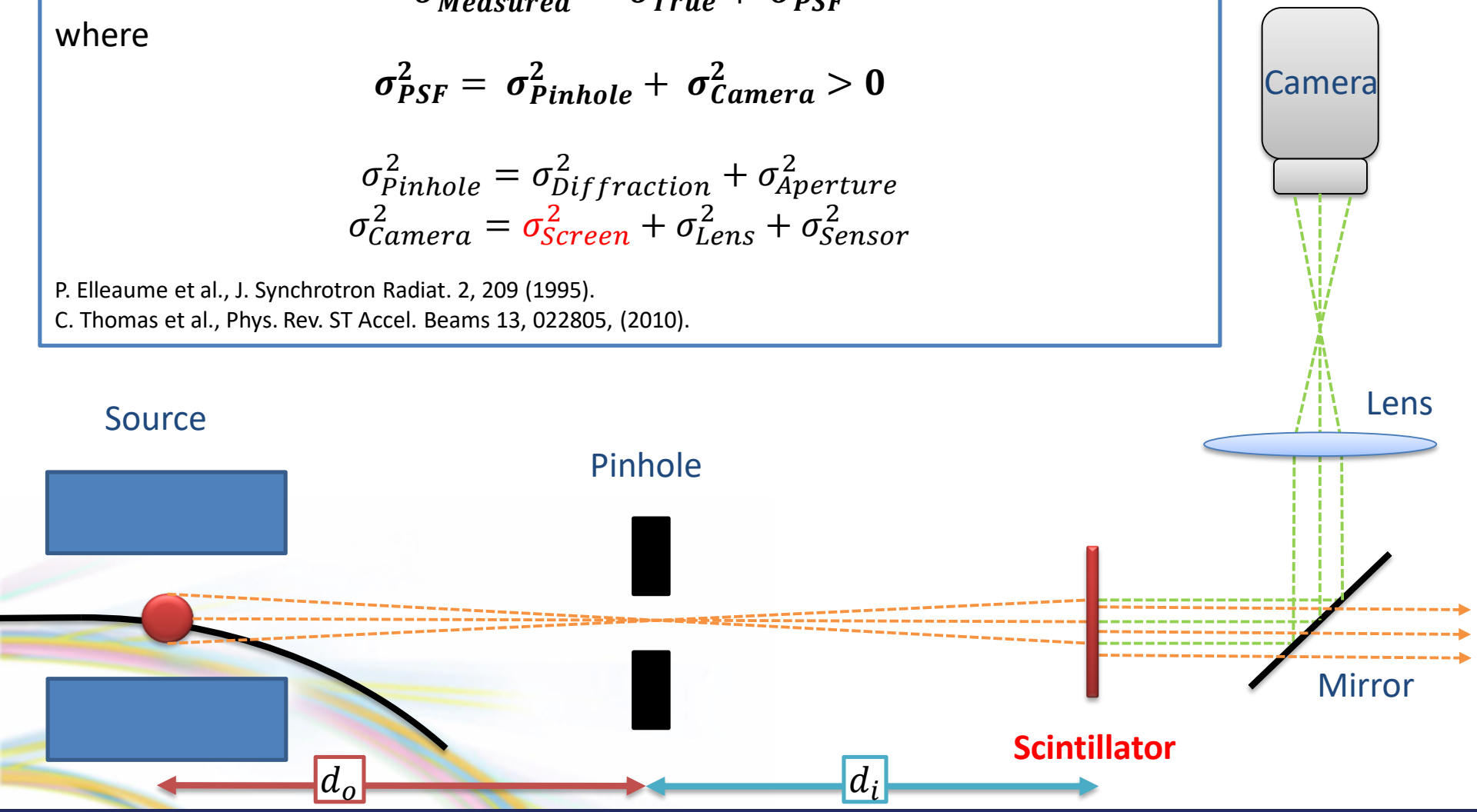

Reducing Scintillator Contribution to PSF

Spatial resolution is improved by reducing the scintillator thickness.

G. Kube et al., Proc. IBIC2015, Melbourne, Australia, p.330

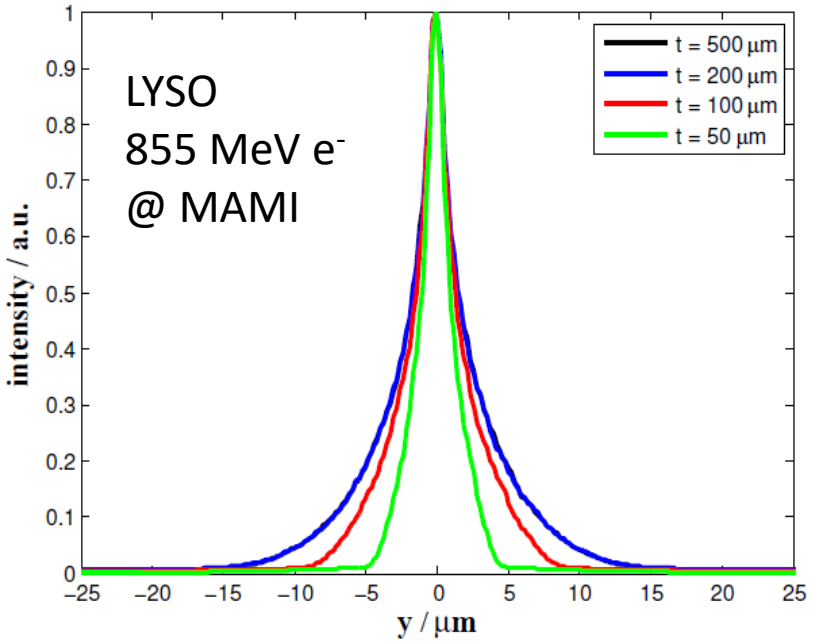

Figure 8: Simulated SPFs for different scintillator thicknesses. The simulations were performed for NA = 0.20 and λ = 420 nm.

SPF = Single Particle Resolution Function

$$\text{Contrast} = \frac{I_{\max} - I_{\min}}{I_{\max} + I_{\min}}$$

P.-A Douissard et al., 2012 JINST 7 P09016

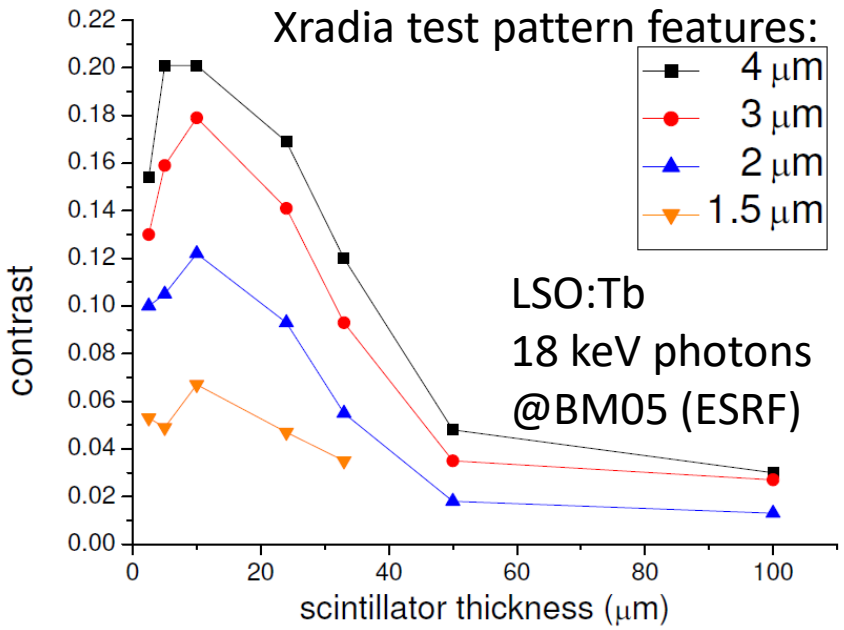

Figure 6. Influence of the thickness of the single crystal scintillator film on the contrast achievable in the image with a 10× (NA = 0.4) microscope objective (18 keV photon energy, different graphs represent results obtained by using differently sized features in the Xradia test pattern).

Dependence of Photon Yield

Spatial resolution is improved by reducing the scintillator thickness. However, a thin scintillator will emit fewer photons.

$$I = I_o e^{-t/\mu}$$

I_o = incoming intensity, I=outgoing intensity, μ= attenuation length, t=thickness

M. Ishii and M. Kobayashi, Prog. Crystal Growth and Charact. 1991, 23, 245-311

Table 1

M. Rutherford et al., J. Synchrotron Rad. (2016). 23, 685-693

Scintillator materials for hard X-ray detection on the sub-μs timescale.

Crystal	Density (g cm^{-3})	Emission maximum (nm)	Attenuation length (25 keV, 50 keV) (μm)	Light yield (photons MeV^{-1})	Dominant decay time (ns)
$Cs_2NaYBr_3I_3$:Ce	4.0	425	125, 252	43000	43
$Cs_2NaLaBr_3I_3$:Ce	4.0	438	138, 229	58000	68
$Cs_2LiLaBrCl$:Ce	4.1	419	143, 215	50000	55
K_2LaI_5:Ce	4.4	450	166, 195	52000	24
YAG:Ce†	4.6	550	122, 791	24000	96
YI_3:Ce	4.6	532	117, 176	99000	34
$Gd_3Al_2Ga_3O_{12}$:Ce	4.7	550	124, 869	55000	60
$RdGd_2Br_7$:5%Ce	4.7	430	77, 508	42000	45
GdI_3:5%Ce	5.2	552	114, 195	83000	33
LuI_3:Ce	5.6	540	91, 176	115000	33
$Lu_3Al_5O_{12}$:Ce†	6.7	525	66, 405	27000	61
$(LuY)Si_2O_5$:Ce†	7.1	420	75, 461	34000	41
$SrHfO_3$:Ce	7.6	410	45, 284	40000	42
$BaHfO_3$:Ce	8.5	400	52, 148	40000	25

Microscope Objective

Therefore, the optical system must have a large numerical aperture (NA) to capture as many photons as possible from the thin scintillator.

Reflective Microscope Objective

- To **avoid browning from X-ray** exposure a reflective objective is used.
- For optimal spatial resolution, the **scintillator thickness must be matched to the NA** of the microscope objective.
- Not a novel idea! Commercially available ~£30k predominantly for beamlines. **It's now possible to build in-house at a fraction of the cost** since reflective objectives are available from Thorlabs and Newport.

A. Koch et al., J. Opt. Soc. Am., (15) 7, 1998

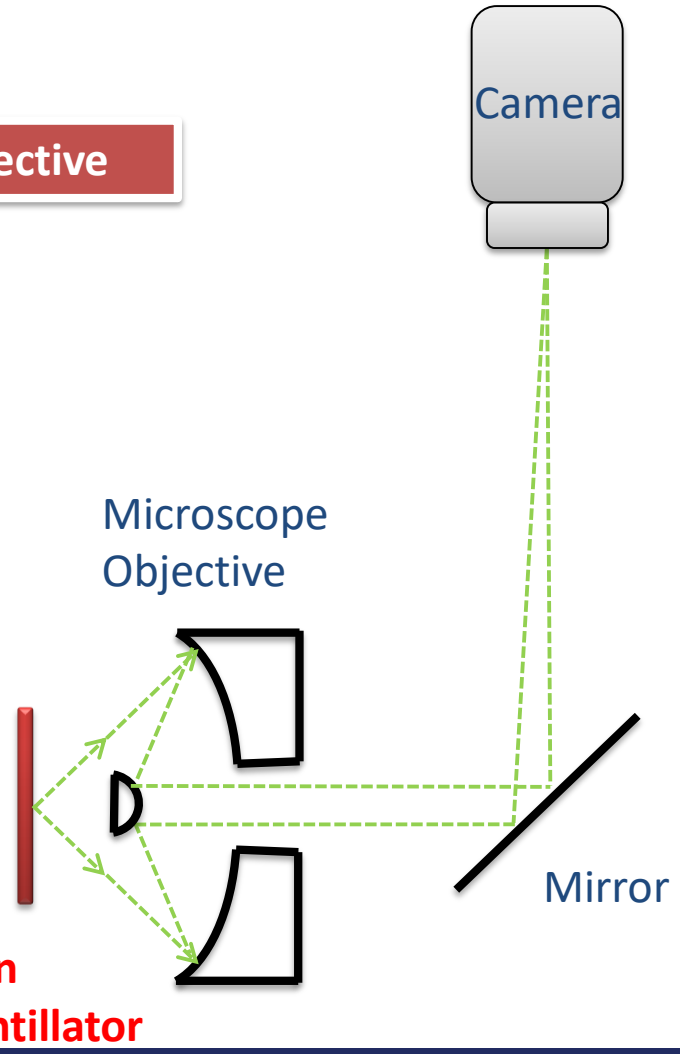

Lens Comparison in Lab

Refractive

For thick (200µm) scintillator

	REFRACTIVE LENS	REFLECTIVE MICROSCOPE OBJECTIVE
F-number	2.8 to 8	1.25*
Numerical Aperture	0.18 to 0.06*	0.4
Focal length	50.2 mm	160 mm (back) 13 mm (effective)
Working distance	-	24 mm
Magnification	1	15
Transmission	400-700 nm	200-1000 nm

Reflective

For thin (<50µm) scintillator

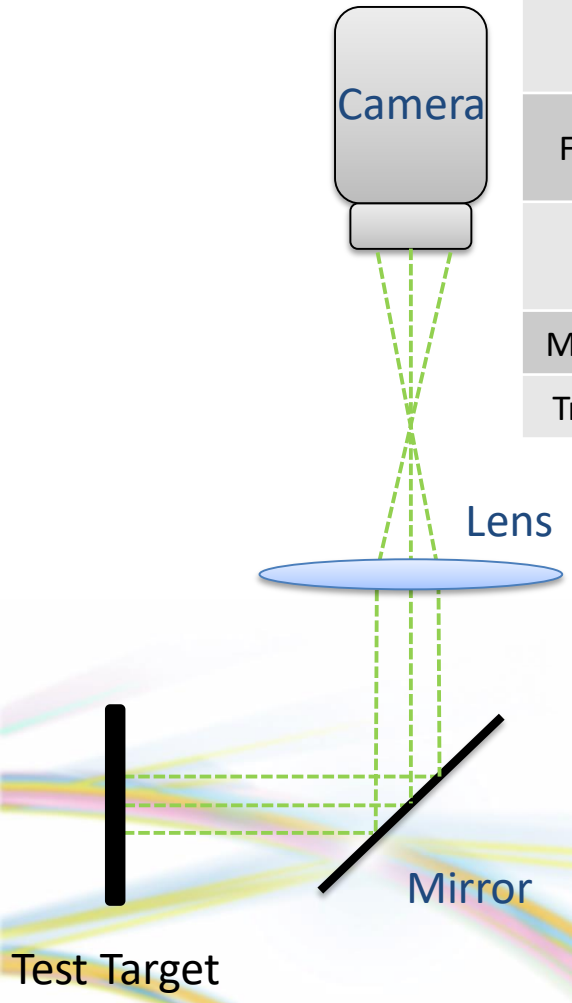

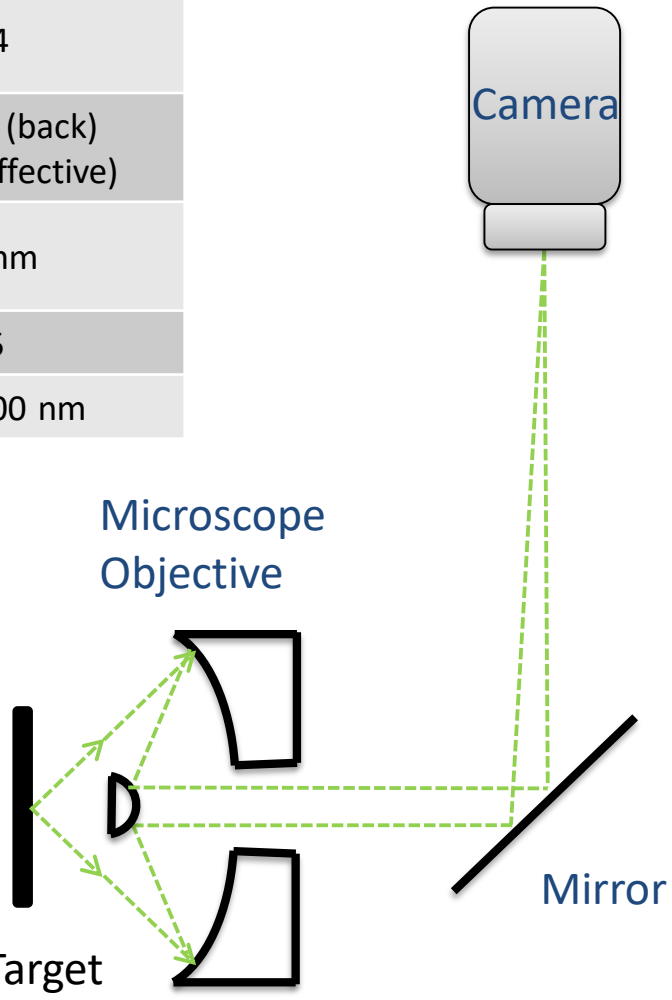

Modulation Transfer Function

The MTF (or spatial frequency response) is the magnitude response of the optical system to sinusoids of different spatial frequencies.

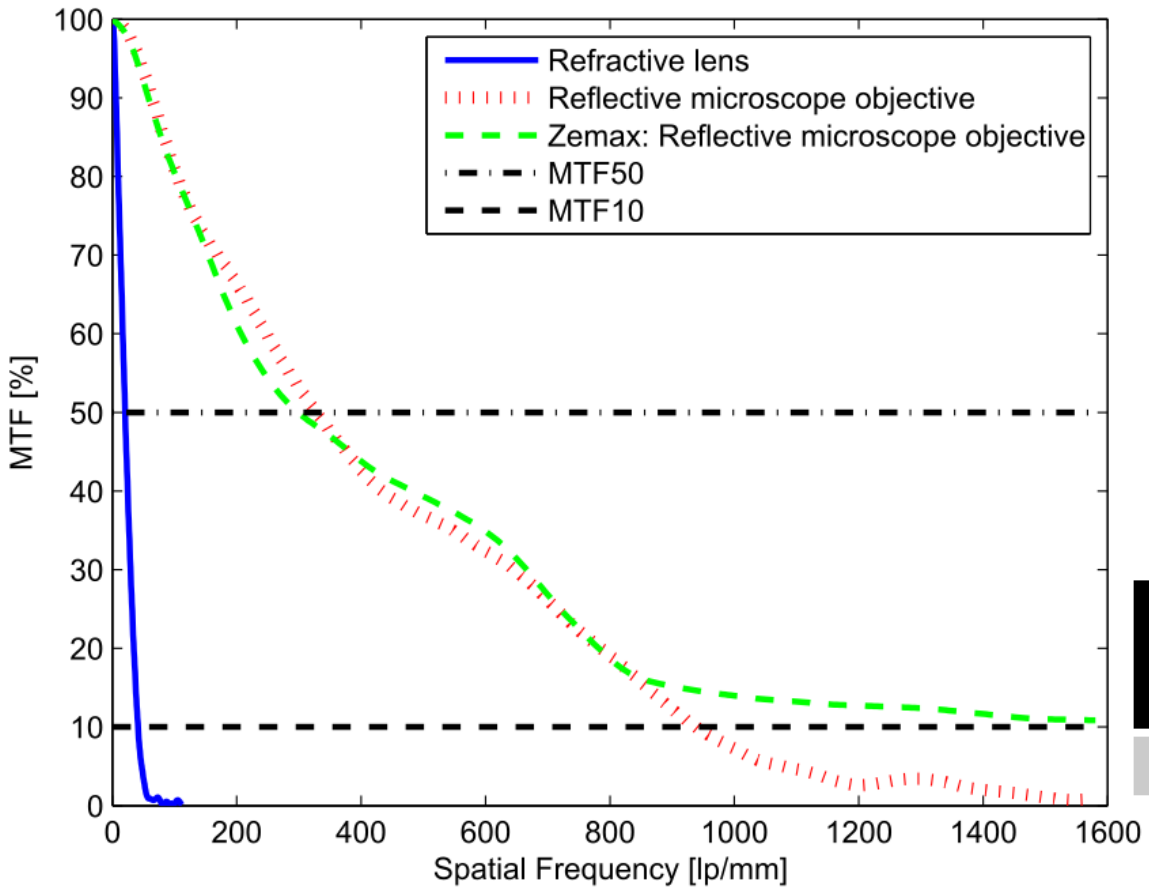

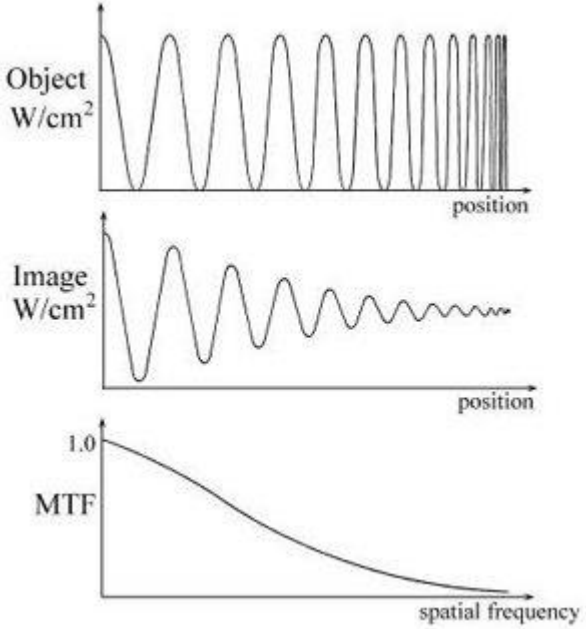

	REFRACTIVE LENS	REFLECTIVE MICROSCOPE OBJECTIVE
MTF10	42 lp/mm	936 lp/mm

G.D. Boreman, "Modulation Transfer Function in Optical and Electro-Optical Systems", SPIE Press, Bellingham, WA (2001)
www.thorlabs.com

Comparison of Thick vs Thin Scintillator + Optics

Ideally, the **scintillator contribution to the PSF** would be measured **using the knife-edge** technique with X-ray exposure.

However a suitable X-ray knife-edge was not available in time for these tests.

Instead, we **measured the total PSF** of each system **using the Touschek lifetime** as a proxy for true vertical beam size.

Refractive

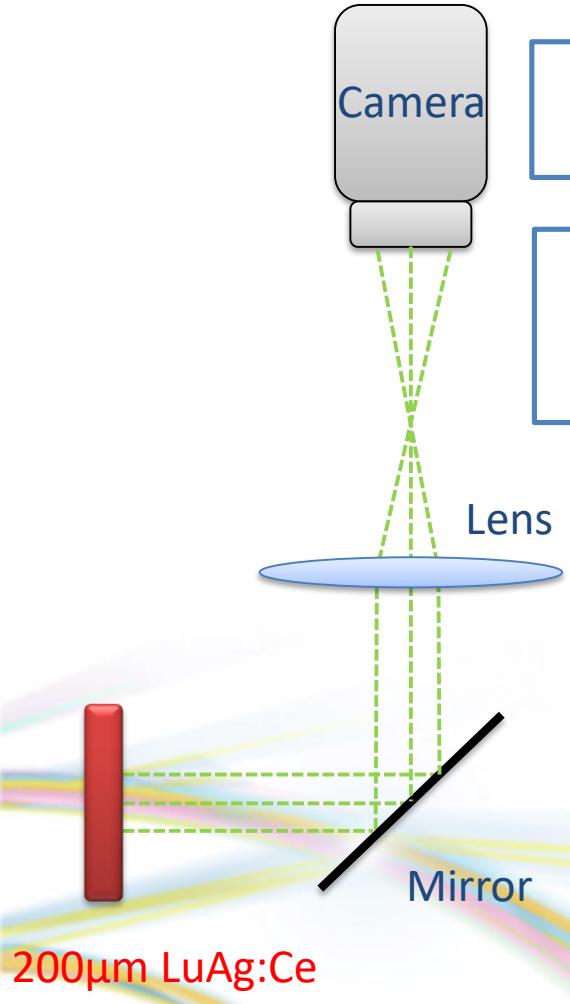

Reflective

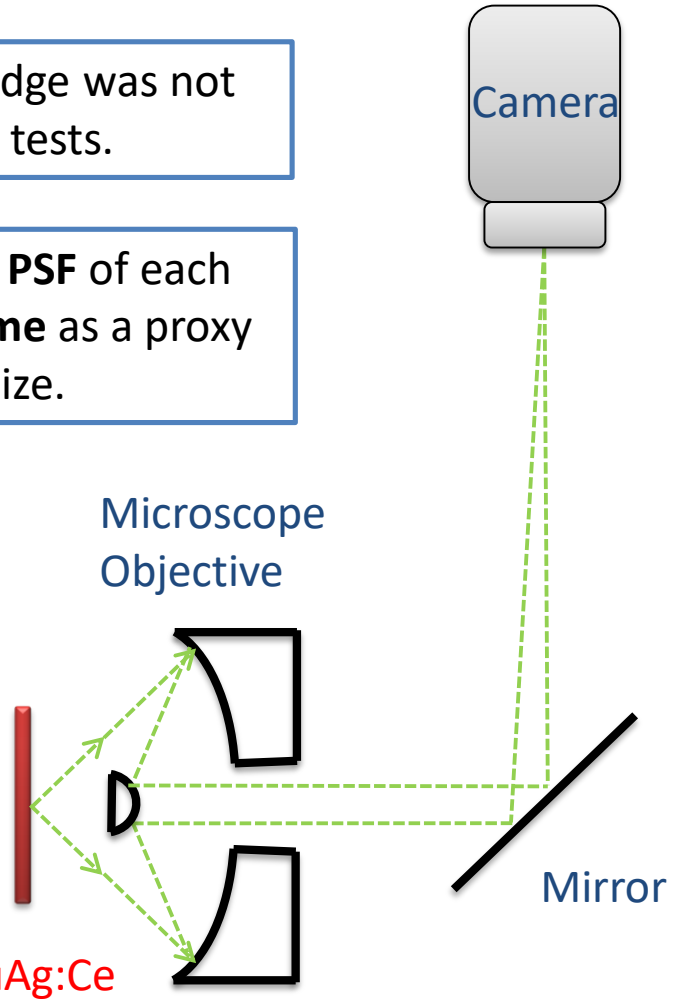

PSF Measurement using Touschek Lifetime

In the **Touschek dominated regime** (400 bunch, 200 mA) the measured **beam lifetime** (or condition) τ **is used as a proxy measurement for the true beam size** σ_y as:

$$\sigma_y = k\tau \tag{1}$$

where k is a scaling factor.

Subtraction in quadrature given a Gaussian beam profile and PSF σ_{PSF} gives the measured beam size σ_M as:

$$\sigma_M = \sqrt{\sigma_y^2 + \sigma_{PSF}^2} \tag{2}$$

Substituting Eq. (1) into (2):

$$\boldsymbol{\sigma_M = \sqrt{(k\tau)^2 + \sigma_{PSF}^2}} \tag{3}$$

A. Piwinski, "The Touschek effect in strong focusing storage rings", DESY 98-179, 1998
L.M. Bobb et al., Proc. of IBIC2016, Barcelona, Spain, WEPG63.

Experiment

The refractive and reflective microscope imagers were installed on X-ray pinhole camera 3 in the storage ring tunnel to ensure all other PSF contributions are identical.

X-ray Pinhole Camera	Scintillator	Source-to-scintillator magnification	Scintillator-to-camera magnification	Optical setup
1	200 µm Prelude 420: LYSO:Ce	2.39	1	**Refractive lens**
2		2.65	1	
3	**200 µm LuAg:Ce**	**2.47**	**1**	
	25 µm LuAg:Ce		**11**	**Microscope**

Since the two setups on pinhole 3 could not be calibrated simultaneously, X-ray pinhole cameras 1 and 2 were used to verify that the beam conditions did not change between the consecutive PSF measurements using the Touschek lifetime.

L. Bobb and G. Rehm, Proc. of IBIC2018, Shanghai, China, WEPB18.

PSF results (1)

L. Bobb and G. Rehm, Proc. of IBIC2018, Shanghai, China, WEPB18.

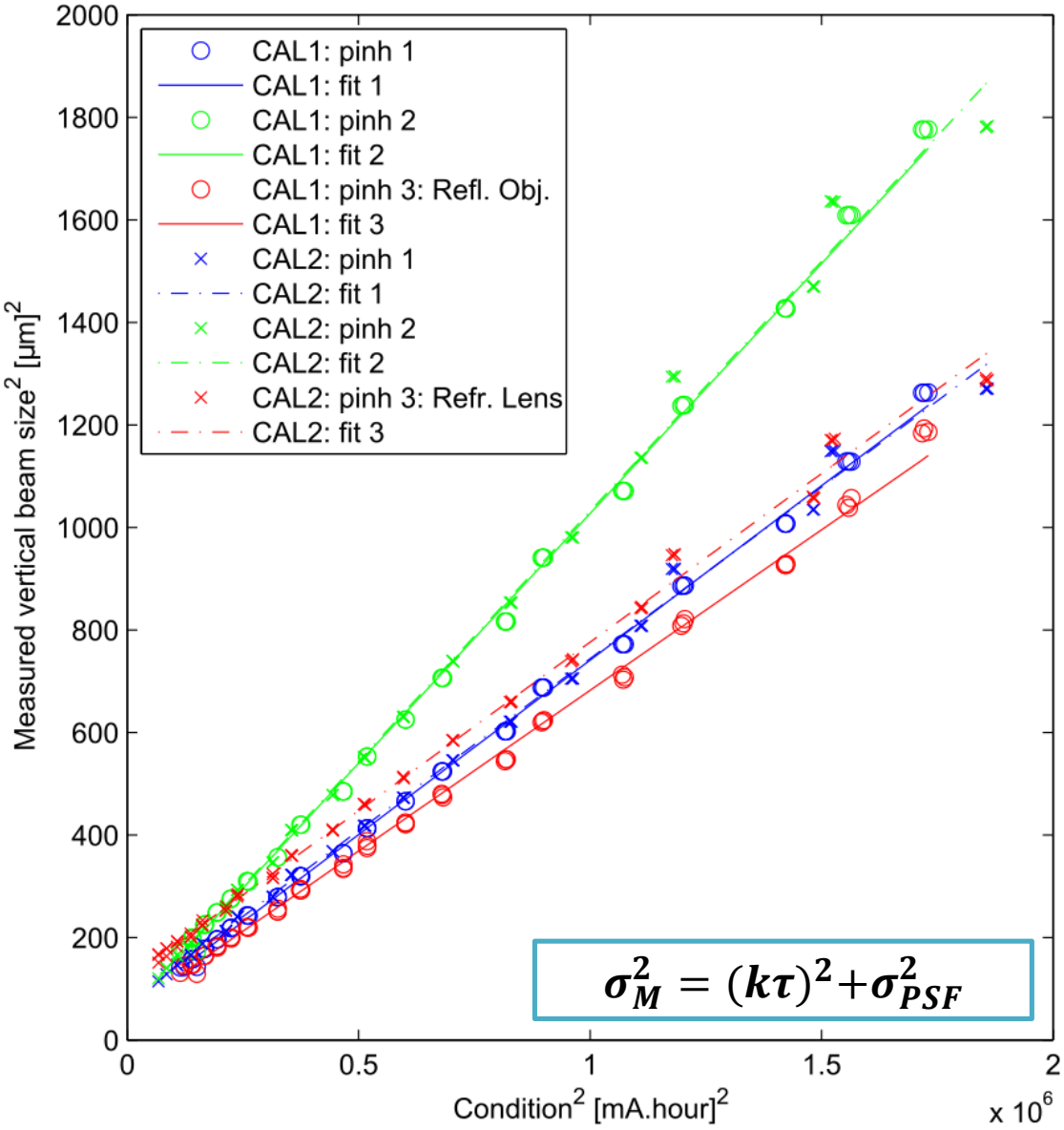

PSF results (2)

PINHOLE CAMERA	CALIBRATION 1		CALIBRATION 2	
	k [µm mA^{-1} h^{-1}]	σ_{PSF} [µm]	k [µm mA^{-1} h^{-1}]	σ_{PSF} [µm]
1	0.026	7.8	0.026	8.6
2	0.031	7.2	0.031	7.5
	Reflective microscope imager with thin 25µm scintillator		Refractive lens imager with thick 200µm scintillator	
3	0.025	**7.4**	0.026	**10.9**

Using a thin scintillator resulted in a 30% improvement to total PSF

L. Bobb and G. Rehm, Proc. of IBIC2018, Shanghai, China, WEPB18.